

# Carbon dioxide reforming of methane over co-precipitated Ni–CeO<sub>2</sub>, Ni–ZrO<sub>2</sub> and Ni–Ce–ZrO<sub>2</sub> catalysts

Hyun-Seog Roh, H.S. Potdar, Ki-Won Jun\*

Chemical Technology Division, Korea Research Institute of Chemical Technology, P.O. Box 107, Yuseong, Daejeon 305-600, Republic of Korea

Available online 2 July 2004

## Abstract

A co-precipitation method was employed to prepare nickel oxide dispersed on CeO<sub>2</sub>, ZrO<sub>2</sub> and cubic Ce<sub>0.8</sub>Zr<sub>0.2</sub>O<sub>2</sub> support to obtain catalysts useful for carbon dioxide reforming of methane reaction. The Ni–CeO<sub>2</sub> and Ni–Ce–ZrO<sub>2</sub> catalysts showed relatively high activity and stability, while the Ni–ZrO<sub>2</sub> catalyst deactivated in the initial stage of the reaction due to serious carbon formation. The co-precipitated Ni–Ce–ZrO<sub>2</sub> catalyst exhibited the highest catalytic activity (CH<sub>4</sub> conversion >97% at 800 °C) among the catalysts tested and the activity was maintained without significant loss during the reaction for 100 h. The enhanced catalytic activity and stability of the co-precipitated Ni–Ce–ZrO<sub>2</sub> catalyst is attributed to the combination of nano-crystalline nature of cubic Ce<sub>0.8</sub>Zr<sub>0.2</sub>O<sub>2</sub> support and finely dispersed nano-sized NiO<sub>x</sub> crystallites resulting in intimate contact between Ni and support, better Ni dispersion, higher Ni surface area and enhanced oxygen transfer during the reaction.

© 2004 Elsevier B.V. All rights reserved.

**Keywords:** Co-precipitation; Cubic Ce–ZrO<sub>2</sub>; CH<sub>4</sub>; CO<sub>2</sub>; Reforming

## 1. Introduction

Recently, much attention has been focused on carbon dioxide reforming of CH<sub>4</sub> (CDR) for the production of synthesis gas owing to both environmental and commercial reasons [1–16]. Supported-Ni catalysts have been tried for this reaction and showed high activity comparable to noble metals [3–6]. However, supported-Ni catalysts deactivate due to either coke formation or sintering of the metallic and support phases [6,7]. The primary difficulty associated with the application of CDR is finding suitable Ni based catalysts having stability under severe conditions [7]. It has been reported that the nature of supports affects the catalytic performance of Ni catalysts in CDR [7]. The activity and stability of these catalysts varied greatly with different supports [7,8].

There has been a lot of interest developed in mixed oxide catalyst system like Ce<sub>1-x</sub>Zr<sub>x</sub>O<sub>2</sub> (Ce–ZrO<sub>2</sub>) because of certain inherent advantages [17]. The co-precipitation method was earlier reported to get better dispersion of Ni in yttrium stabilized zirconia (YSZ) matrix for fuel cell

anode material [18]. It is known that the addition of ZrO<sub>2</sub> to CeO<sub>2</sub> leads to improvements in oxygen storage capacity of CeO<sub>2</sub>, redox property, thermal resistance and promotion of metal dispersion [17–19], resulting in better performance in CO oxidation [20], combustion of methane [21] and NO reduction [22]. Furthermore, it has been established that the reducibility of CeO<sub>2</sub> is greatly enhanced when it is mixed with ZrO<sub>2</sub> to form solid solution of Ce–ZrO<sub>2</sub>. The reduction temperatures as low as 427 °C have been reported for solid solution of Ce–ZrO<sub>2</sub> system during repeated reduction/oxidation cycles [23,24]. Therefore, Ce–ZrO<sub>2</sub> system has appeared as a promising candidate of a support material in nickel based catalyst system. Only limited number of papers are concerned with this objective [25–27]. Lercher et al. [6] reported that Pt/ZrO<sub>2</sub> showed excellent performance in CDR. However, Ni/ZrO<sub>2</sub> with a high Ni loading is not suitable for CDR due to coke formation. Li et al. [26,27] reported that Ni/ZrO<sub>2</sub> catalysts with more than 10 wt.% Ni loading showed high activity at 750 °C for 30 h in CDR in spite of producing a large amount of carbon. However, its stable activity can be obtained only under diluted reaction conditions, namely dilution of reactants with N<sub>2</sub> and dilution of catalysts with quartz sand. Montoya et al. [28] tried Ni based catalyst on a tetragonal Ce–ZrO<sub>2</sub> support mate-

\* Corresponding author. Fax: +82 42 860 7388.

E-mail address: [kwjun@kriect.re.kr](mailto:kwjun@kriect.re.kr) (K.-W. Jun).

rial for CDR; however, the problem of support sintering at 800 °C could not be avoided completely. It has been reported that the cubic phase of Ce–ZrO<sub>2</sub> has more oxygen storage capacity and is more easily reducible than the tetragonal phase [29]. In addition, the co-precipitation method has been reported to get better dispersion of Ni than the conventional impregnation method [30]. In this study, we prepared co-precipitated Ni–CeO<sub>2</sub>, Ni–ZrO<sub>2</sub> and Ni–Ce–ZrO<sub>2</sub> catalysts and examined their catalytic activity for CDR. We report here that the co-precipitated Ni–Ce–ZrO<sub>2</sub> catalysts exhibited remarkably high activity and stability in CDR due to high dispersion of Ni on Ce–ZrO<sub>2</sub>.

## 2. Experimental

### 2.1. Catalyst preparation

Ni–CeO<sub>2</sub>, Ni–ZrO<sub>2</sub> and Ni–Ce<sub>0.8</sub>–Zr<sub>0.2</sub>O<sub>2</sub> catalysts were prepared by a co-precipitation method. Ni content was fixed at 15 wt.%. In the case of Ni–Ce<sub>0.8</sub>–Zr<sub>0.2</sub>O<sub>2</sub> (Ni–Ce–ZrO<sub>2</sub>), Ce–ZrO<sub>2</sub> comprised 80 mol% of CeO<sub>2</sub> and 20 mol% of ZrO<sub>2</sub>. Stoichiometric quantities of zirconyl nitrate solution (20 wt.% in ZrO<sub>2</sub> base, MEL Chemicals), cerrous nitrate (99.9%, Aldrich) and nickel nitrate (97%, Junsei Chemicals) were dissolved in distilled water, and the resulting solution was transferred to a round bottom flask. To this solution an aqueous solution of 20% KOH (w/w) was added drop-wise at 80 °C with constant stirring to attain a pH of 10.5. During the entire course of co-precipitation reactions, the pH was maintained. The precipitates were digested at 80 °C for 72 h. Later, they were thoroughly washed with distilled water several times to remove any potassium impurity and then initially air-dried for 48 h followed by drying at 120 °C for 6 h. The dried mass thus obtained was then finely ground to a particle size less than a micron. This material was finally calcined at 800 °C for 6 h in an aerobic environment to get the final catalyst. Simultaneously, for comparison, Ni/CeO<sub>2</sub>, Ni/ZrO<sub>2</sub> and Ni/Ce–ZrO<sub>2</sub> catalysts (Ni = 15%, w/w) were prepared by the conventional impregnation method. This was achieved by impregnating appropriate amounts of Ni(NO<sub>3</sub>)<sub>2</sub>·6H<sub>2</sub>O onto supports (CeO<sub>2</sub>, ZrO<sub>2</sub> and Ce–ZrO<sub>2</sub>) which were prepared by the co-precipitation methodology described above but with the omission of the nickel source. The impregnated catalysts were dried and calcined in the same way as the co-precipitated ones.

### 2.2. Characterization

The BET specific surface area was measured by nitrogen adsorption at –196 °C using a Micromeritics (ASAP-2400) surface area measurement apparatus. The XRD patterns were recorded using a Rigaku 2155D6 diffractometer (Ni filtered Cu–K $\alpha$  radiation, 40 kV, 50 mA). Pulse chemisorptions were performed in a flow apparatus. About 200 mg of catalyst

was placed in a quartz reactor. Before pulse chemisorption, the sample was reduced in 5% H<sub>2</sub>/Ar at 700 °C for 3 h. Then the sample was purged in Ar at 720 °C for 1 h and cooled to 50 °C in flowing Ar. Hydrogen was pulsed over the catalyst to measure the chemisorption at 50 °C using 5% H<sub>2</sub>/Ar and continued at 8 min intervals until the area of the hydrogen peak on the chromatograph was identical. Based on the hydrogen uptake, the surface area of Ni was calculated by assuming the adsorption stoichiometry of one hydrogen atom per nickel surface atom (H/Ni<sub>s</sub> = 1).

### 2.3. Catalytic reaction

Activity tests were carried out using a fixed-bed micro-reactor [30,31]. The reactant feed comprised a gaseous mixture of CH<sub>4</sub>:CO<sub>2</sub>:N<sub>2</sub> (1.00:1.04:1.00). N<sub>2</sub> was employed as the reference for calculating CH<sub>4</sub> and CO<sub>2</sub> conversions. Each catalyst was reduced in the reactor with 5% H<sub>2</sub>/N<sub>2</sub> at 700 °C for 3 h prior to each catalytic activity measurement. The catalytic reactions were executed at the condition of  $T = 800$  °C and GHSV = 108,000 ml/h g unless otherwise stated. Effluent gases from the reactor were analyzed by a gas chromatograph (Chrompack CP9001) fitted with a fused silica capillary column (CarboPLOT P7) equipped with a thermal conductivity detector (TCD).

## 3. Results and discussion

### 3.1. Characterization

In our previous research, many synthesis parameters such as pH, digestion time, addition sequence, use of tetrapropyl ammonium bromide, i.e. TPABr (4.3 wt.%) were systematically varied in the co-precipitation method [30]. Hence, optimized co-precipitation condition to obtain high surface area materials was achieved by the addition of 20% KOH to an aqueous solution containing a stoichiometric concentrations of cerium, zirconium and nickel nitrates for a digestion time of 72 h at 80 °C. It was also found that 15% Ni loading is the optimum Ni loading amount to achieve high activity and high stability in CDR.

For the screening purpose in CDR, three catalysts with the same 15% Ni loading on CeO<sub>2</sub>, ZrO<sub>2</sub> and Ce<sub>0.8</sub>Zr<sub>0.2</sub>O<sub>2</sub> supports were prepared by the co-precipitation method. Characteristics of supports and catalysts are summarized in Table 1. All the supports and catalysts were calcined at 800 °C for 6 h. Among the supports, the Ce<sub>0.8</sub>Zr<sub>0.2</sub>O<sub>2</sub> shows the highest BET surface area, indicating that the cubic Ce–ZrO<sub>2</sub> has higher BET surface area than CeO<sub>2</sub> or ZrO<sub>2</sub>. Compared with the supports, the co-precipitated Ni catalysts show higher BET surface areas. This suggests that Ni incorporation results in the development of fine structure. The Ni surface areas estimated from H<sub>2</sub> chemisorption increase in the order: Ni–CeO<sub>2</sub> < Ni–ZrO<sub>2</sub> < Ni–Ce<sub>0.8</sub>Zr<sub>0.2</sub>O<sub>2</sub>. Both BET surface area and Ni surface area indicate that Ni is

Table 1  
Characteristics of supports and catalysts prepared by co-precipitation method

Ni content (wt.%)	Support	Surface area (m <sup>2</sup> /g) <sup>a</sup>	Ni surface area (m <sup>2</sup> /g) <sup>b</sup>	Support size (nm) <sup>c</sup>	NiO size (nm) <sup>d</sup>
0	CeO <sub>2</sub>	9	—	7.3	—
0	ZrO <sub>2</sub>	37	—	12.3	—
0	Ce <sub>0.8</sub> Zr <sub>0.2</sub> O <sub>2</sub>	89	—	5.9	—
15	CeO <sub>2</sub>	40	0.37	9.8	NA <sup>e</sup>
15	ZrO <sub>2</sub>	54	0.81	10.3	7.7
15	Ce <sub>0.8</sub> Zr <sub>0.2</sub> O <sub>2</sub>	92	1.93	6.5	NA <sup>e</sup>

<sup>a</sup> Estimated from N<sub>2</sub> adsorption at −196 °C.

<sup>b</sup> Estimated from H<sub>2</sub> chemisorption at 50 °C.

<sup>c</sup> Estimated from XRD.

<sup>d</sup> Estimated from XRD.

<sup>e</sup> Not available due to very broad and weak XRD peaks.

well dispersed onto Ce<sub>0.8</sub>Zr<sub>0.2</sub>O<sub>2</sub> resulting in the highest BET surface area and Ni surface area of the catalyst.

The XRD patterns for Ni–CeO<sub>2</sub>, Ni–ZrO<sub>2</sub> and Ni–Ce<sub>0.8</sub>Zr<sub>0.2</sub>O<sub>2</sub> are given in Fig. 1. The 15% Ni–CeO<sub>2</sub> catalyst gave all characteristic reflections corresponding to (1 1 1), (2 0 0), (2 2 0), (3 1 1), (2 2 2) and (4 0 0) planes. The NiO peaks observed are very broad indicating thereby good dispersion of NiO crystallites in CeO<sub>2</sub> matrix. On the other hand, the 15% Ni–ZrO<sub>2</sub> catalyst showed all characteristic reflections corresponding to reported tetragonal structure of ZrO<sub>2</sub>. The NiO crystallite size calculated by Scherrer equation is found to be 7.7 nm and the support size of ZrO<sub>2</sub> is 10.3 nm. In the case of 15% Ni–Ce<sub>0.8</sub>Zr<sub>0.2</sub>O<sub>2</sub> catalyst, XRD pattern showed all reflections corresponding to the cubic Ce–ZrO<sub>2</sub> solid solution with the lattice parameter of 5.35 Å. The NiO crystallites are very small as the peaks due to NiO are quite broad. Therefore, NiO crystallite size could not be estimated in this catalyst composition. The XRD results thus confirmed good dispersion of NiO crystallites in the cubic Ce–ZrO<sub>2</sub> matrix. It is noteworthy that high surface area and good dispersion of NiO crystallites in the 15% Ni–Ce<sub>0.8</sub>Zr<sub>0.2</sub>O<sub>2</sub> catalyst is obtained even after calcination at 800 °C. As a consequence,

the Ni–Ce<sub>0.8</sub>Zr<sub>0.2</sub>O<sub>2</sub> catalyst showed higher Ni surface area after reduction with 5% H<sub>2</sub>/N<sub>2</sub> at 700 °C for 3 h.

The BET surface area of the impregnated Ni/Ce–ZrO<sub>2</sub> catalyst after calcination at 800 °C for 6 h was 50 m<sup>2</sup>/g, indicating significant decrease of surface area after impregnation of Ni onto Ce–ZrO<sub>2</sub>. Thus, the comparison of BET surface area between the co-precipitated Ni–Ce–ZrO<sub>2</sub> and impregnated Ni/Ce–ZrO<sub>2</sub> catalysts clearly confirms that the co-precipitation method is more effective to prepare high surface area catalysts than the conventional impregnation method.

The XRD patterns for the co-precipitated and impregnated catalysts before and after reduction treatment are shown for comparison in Fig. 2. All the patterns can be indexed for cubic fluorite structure of Ce<sub>0.8</sub>Zr<sub>0.2</sub>O<sub>2</sub> and show reflections corresponding to (1 1 1), (2 0 0), (2 2 0), (3 1 1), (2 2 2) and (4 0 0) planes. No line corresponding to either ZrO<sub>2</sub> or CeO<sub>2</sub> is observed. Thus, the XRD analyses show that a cubic Ce<sub>0.8</sub>Zr<sub>0.2</sub>O<sub>2</sub> solid solution is formed by the co-precipitation method and calcination at 800 °C for 6 h. The similarity of our measured lattice parameters to those from reference materials further confirms the formation of solid solution of

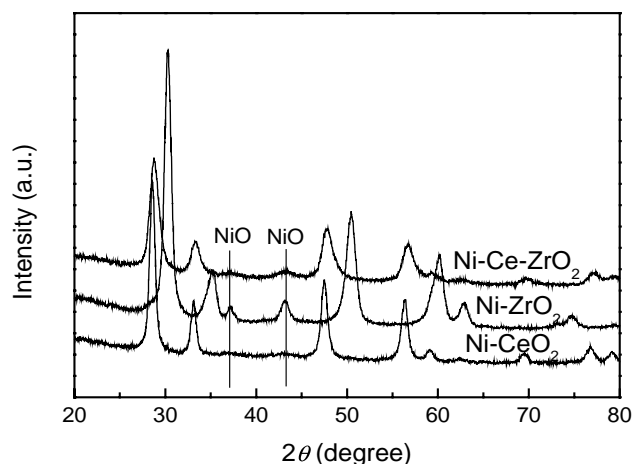


Fig. 1. XRD patterns of co-precipitated Ni–CeO<sub>2</sub>, Ni–ZrO<sub>2</sub> and Ni–Ce<sub>0.8</sub>Zr<sub>0.2</sub>O<sub>2</sub> catalysts.

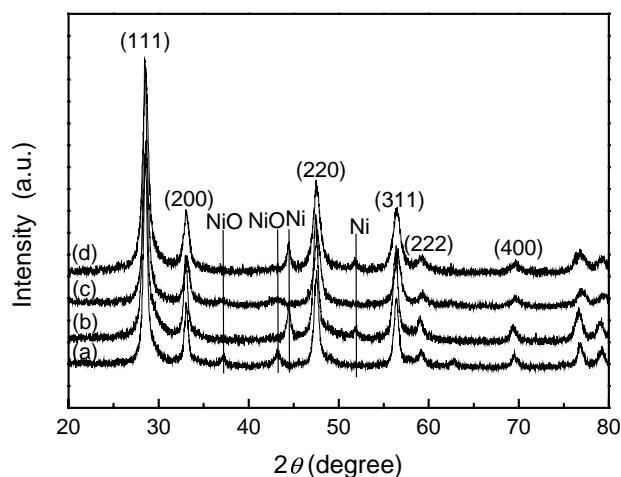


Fig. 2. XRD patterns of Ni–Ce–ZrO<sub>2</sub> catalysts: (a) fresh impregnated catalyst, (b) reduced impregnated catalyst, (c) fresh co-precipitated catalyst, (d) reduced co-precipitated catalyst.

cubic  $\text{Ce}_{0.8}\text{Zr}_{0.2}\text{O}_2$  in the present case [32,33]. The other reflections observed at  $2\theta$  values equal to  $37.21^\circ$ ,  $43.21^\circ$ , and  $62.73^\circ$  are assigned to cubic NiO with  $a_0 = 4.176 \text{ \AA}$  [34]. The analysis of these XRD patterns indicated a shift in the reflections towards higher angles for all the peaks due to insertion of smaller  $\text{Zr}^{4+}$  ions in the lattice of  $\text{CeO}_2$ . The XRD patterns clearly indicated the presence of cubic  $\text{Ce}_{0.8}\text{Zr}_{0.2}\text{O}_2$  phase having better dispersion of cubic NiO particles in the matrix. Thus, higher surface area of the co-precipitated material is due to the fine nano-sized crystallites of the  $\text{Ce}_{0.8}\text{Zr}_{0.2}\text{O}_2$  particles. Furthermore, the NiO peaks in the co-precipitated catalyst are much broader than those in impregnated one, indicating thereby better dispersion and less sintering of fine NiO particles during the calcination process. The NiO crystallite size of the co-precipitated catalyst could not be estimated because of very broad and weak peaks while the size of impregnated one was estimated to be 8.5 nm. It is quite reasonable to assume that the NiO crystallite size of the co-precipitated catalyst is less than 3 nm, which corresponds to the limitation of X-ray line broadening analysis.

After a reduction treatment with 5%  $\text{H}_2/\text{N}_2$  at  $700^\circ\text{C}$  for 3 h, crystallite sizes of Ni of the co-precipitated and impregnated catalysts were 10.5 and 11.6 nm, respectively. In the case of the impregnated catalyst, the size change from NiO to Ni particles is about 3 nm after the reduction process. On the contrary, the co-precipitated catalyst showed relatively higher difference (from less than 3 to 10.5 nm) after the reduction treatment. It is likely that some parts of the agglomerated particles of the co-precipitated catalysts were detected, while the other parts containing relatively fine small particles could not be detected in XRD after the reduction process. This postulation is supported by the Ni surface area obtained from  $\text{H}_2$  chemisorption. BET surface areas and crystallite sizes of  $\text{Ce}_{0.8}\text{Zr}_{0.2}\text{O}_2$  in both catalysts were kept to the same values after the reduction treatment. The values of  $\text{H}_2$  uptake of the co-precipitated and impregnated catalysts were 23.67 and  $7.44 \mu\text{mol/g}_{\text{cat}}$ , respectively. The Ni surface areas for both catalysts were 1.93 and  $0.61 \text{ m}^2/\text{g}$ , respectively. This clearly indicates that the co-precipitated catalyst has better Ni dispersion than impregnated one even after the reduction process. Besides, the peak appearing at  $2\theta = 51.80$  corresponding to (200) reflection with  $d = 1.7647 \text{ \AA}$  for Ni metal in the co-precipitated catalyst was broader than that observed in impregnated one. This observation also indicates that better Ni dispersion was maintained in the co-precipitated catalyst in comparison to the impregnated one after the reduction treatment. The calculated lattice parameter of metallic nickel particles is  $3.525 \text{ \AA}$ , which is in agreement with reported lattice parameter of face centered cubic phase of nickel  $a_0 = 3.523 \text{ \AA}$ .

### 3.2. Reaction results

First, CDR was carried out over the impregnated Ni/ $\text{CeO}_2$ , Ni/ $\text{ZrO}_2$  and Ni/Ce– $\text{ZrO}_2$  catalysts. All the impregnated cat-

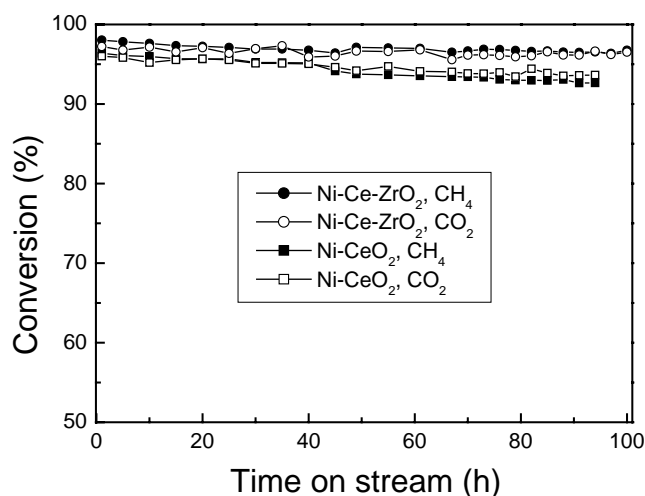


Fig. 3.  $\text{CH}_4$  and  $\text{CO}_2$  conversion with time on stream over co-precipitated Ni– $\text{CeO}_2$  and Ni–Ce– $\text{ZrO}_2$  catalysts ( $T = 800^\circ\text{C}$ , GHSV =  $108,000 \text{ ml/h g}$ ).

alysts did not show stabilities. The impregnated Ni/ $\text{CeO}_2$  and Ni/ $\text{ZrO}_2$  catalysts gave serious coke formation in the initial stage of the reaction. Only Ni/Ce– $\text{ZrO}_2$  showed an initial  $\text{CH}_4$  conversion of 80% and it decreased to 65% within 2 h. Thus, it was confirmed that the conventional impregnation method was not effective to prepare catalysts having good stability in CDR.

The  $\text{CO}_2$  reforming reaction data over the co-precipitated Ni– $\text{CeO}_2$  and Ni–Ce– $\text{ZrO}_2$  catalysts are presented in Fig. 3. Both catalysts exhibited very high activities. On the contrary, CDR could not be carried out over the Ni– $\text{ZrO}_2$  catalyst due to serious carbon formation resulting in blocking the reactor. This is probably relevant to the fact that the Ni– $\text{ZrO}_2$  catalyst has negligible oxygen storage capacity [35]. Ni–Ce– $\text{ZrO}_2$  showed conversion (both  $\text{CH}_4$  and  $\text{CO}_2$ ) of more than 97% up to 100 h without significant deactivation. To the best of our knowledge, it is very rare case that supported-Ni catalyst having more than 5% Ni shows such high activity and stability for 100 h under the condition of GHSV =  $100,800 \text{ ml/h g}$  in CDR. In the case of Ni– $\text{CeO}_2$ , the initial  $\text{CH}_4$  conversion was 1% lower than that of Ni–Ce– $\text{ZrO}_2$ . It is noteworthy that the catalytic activity of Ni– $\text{CeO}_2$  is almost same as that of Ni–Ce– $\text{ZrO}_2$ , even though the Ni surface area of the former is about five times lower than that of the latter. In terms of turnover frequency, Ni– $\text{CeO}_2$  would be more active than Ni–Ce– $\text{ZrO}_2$ . However,  $\text{CH}_4$  conversion after 95 h was 4% lower than that of Ni–Ce– $\text{ZrO}_2$ . It suggests that Ni–Ce– $\text{ZrO}_2$  is more stable than Ni– $\text{CeO}_2$ , indicating that the addition of  $\text{ZrO}_2$  to  $\text{CeO}_2$  stabilizes the catalyst during CDR. This is also supported by the high surface area of the cubic Ce– $\text{ZrO}_2$  support compared with  $\text{CeO}_2$  or  $\text{ZrO}_2$  alone even after calcination at  $800^\circ\text{C}$  for 6 h (Table 1). According to the reaction results, it is clear that  $\text{CeO}_2$  is one of the promising supports in CDR and the addition of  $\text{ZrO}_2$  to  $\text{CeO}_2$  stabilizes the catalyst further.



Table 2  
Reaction results over co-precipitated Ni–Ce–ZrO<sub>2</sub> catalyst with different GHSV

GHSV (ml/h g <sub>cat</sub> )	CH <sub>4</sub> conversion (%)	CO <sub>2</sub> conversion (%)	H <sub>2</sub> yield (%)	CO yield (%)	H <sub>2</sub> /CO ratio
108000	97	97	95	98	0.97
216000	92	93	91	94	0.98

The detailed reaction results of the co-precipitated Ni–Ce–ZrO<sub>2</sub> catalyst are summarized in Table 2. The co-precipitated Ni–Ce–ZrO<sub>2</sub> catalyst showed both CH<sub>4</sub> and CO<sub>2</sub> conversion of more than 97% up to 100 h without detectable deactivation. As the co-precipitated Ni–Ce–ZrO<sub>2</sub> catalyst exhibited almost the equilibrium values of CH<sub>4</sub> and CO<sub>2</sub> conversion, GHSV was doubled (216,000 ml/h g) to avoid equilibrium-limited condition. However, still high CH<sub>4</sub> conversion (92%) and CO<sub>2</sub> conversion (93%) were obtained and the stability was maintained during the reaction time tested. H<sub>2</sub> yields were slightly lower than CH<sub>4</sub> conversions but CO yields were slightly higher than CO<sub>2</sub> conversions. This suggests that RWGS (H<sub>2</sub> + CO<sub>2</sub> → H<sub>2</sub>O + CO) occurred with CDR. As a result, the H<sub>2</sub>/CO ratio was 0.97–0.98, which is very slightly lower than unity. In the case of the impregnated catalyst, both CH<sub>4</sub> and CO<sub>2</sub> conversion were initially about 80% but they decreased to about 65% within 2 h [30].

It is quite probable that the remarkable activity and stability of the co-precipitated Ni–Ce–ZrO<sub>2</sub> catalyst is related to high surface area, nano-crystalline nature of cubic Ce<sub>0.8</sub>Zr<sub>0.2</sub>O<sub>2</sub> support, better dispersion of fine NiO particles in Ce<sub>0.8</sub>Zr<sub>0.2</sub>O<sub>2</sub> support resulting in high Ni surface area, intimate contact between Ni and support, and enhanced oxygen transfer during the CDR. The high surface area is maintained due to agglomeration of primary particles during digestion and strengthening of network structure giving a porous matrix, resulting in withstanding thermal treatment in high temperatures [36]. Consequently, the high surface area was retained in the co-precipitated Ni–Ce–ZrO<sub>2</sub> catalyst after calcination at 800 °C for 6 h. In addition, fine nano-particles of NiO are dispersed onto cubic Ce<sub>0.8</sub>Zr<sub>0.2</sub>O<sub>2</sub> support. As a result, there is very close contact between Ni and support. This would probably enhance oxygen transfer from cubic Ce<sub>0.8</sub>Zr<sub>0.2</sub>O<sub>2</sub> support to Ni, which is beneficial to prevent carbon formation during the CDR. This may help to increase availability of surface oxygen by release mechanism during the CDR reaction [37]. The XRD and SEM studies confirm that fine uniform NiO<sub>x</sub> crystallites are dispersed in the cubic Ce<sub>0.8</sub>Zr<sub>0.2</sub>O<sub>2</sub> support and have the intimate contact with the support. It is known that the cubic Ce<sub>0.8</sub>Zr<sub>0.2</sub>O<sub>2</sub> solid solution is able to shift between CeO<sub>2</sub> under oxidizing conditions and Ce<sub>2</sub>O<sub>3</sub> under reducing conditions by the rapid reduction/oxidation capability, and the capability of redox couple Ce<sup>4+</sup>–Ce<sup>3+</sup> is enhanced in the cubic solid solution of Ce<sub>0.8</sub>Zr<sub>0.2</sub>O<sub>2</sub> rather than CeO<sub>2</sub> [17]. Thus, oxygen ion vacancies in the cubic Ce<sub>0.8</sub>Zr<sub>0.2</sub>O<sub>2</sub> support have beneficial effects on catalytic activities due to the increase in oxygen mobility. A higher rate of oxygen

transfer helps to keep the metal surface from carbon accumulation. Thus, a balance between Ce<sup>4+</sup> reducibility and oxygen storage capacity/mobility is attained by employing ceria rich solid solution.

In summary, the co-precipitation method is one of the promising methods to prepare highly active and stable Ni–Ce–ZrO<sub>2</sub> catalyst for CDR. CeO<sub>2</sub> is one of the best supports in Ni-based catalysts for CDR and the addition of ZrO<sub>2</sub> to CeO<sub>2</sub> stabilizes the catalyst further.

#### 4. Conclusions

The ability to provide mobile oxygen species from the support to Ni plays an important role in keeping the catalysts from carbon deposition during the CDR. As contrast to ZrO<sub>2</sub>, using CeO<sub>2</sub> as a support gives the rather stable catalyst. Furthermore, the cubic Ce–ZrO<sub>2</sub> support provides more stable catalysts than CeO<sub>2</sub> for Ni-based catalysts because ZrO<sub>2</sub> stabilizes the cubic structure at high temperatures and enhances oxygen storage capacity. The co-precipitation method is more effective to prepare highly active and stable Ni–CeO<sub>2</sub> and Ni–Ce–ZrO<sub>2</sub> catalysts for CDR than the conventional impregnation method. The co-precipitated Ni–Ce–ZrO<sub>2</sub> catalyst has higher BET surface area, smaller nano-crystallite sizes of both Ce<sub>0.8</sub>Zr<sub>0.2</sub>O<sub>2</sub> support and NiO compared with the impregnated one. These advantages result in better dispersion of Ni, higher Ni surface area and enhanced oxygen transfer. Due to above-mentioned superior characteristics, the co-precipitated Ni–Ce–ZrO<sub>2</sub> catalyst exhibits high activity and stability in CDR at 800 °C and GHSV of higher than 100,000 ml/h g.

#### References

- [1] M.C.J. Bradford, M.A. Vannice, *Catal. Rev. -Sci. Eng.* 41 (1999) 1.
- [2] J.R. Rostrup-Nielsen, *Stud. Surf. Sci. Catal.* 81 (1993) 25.
- [3] S.M. Stagg-Williams, F.B. Noronha, G. Fendley, D.E. Resasco, *J. Catal.* 194 (2000) 240.
- [4] J.R. Rostrup-Nielsen, J.H. Bak Hansen, *J. Catal.* 144 (1993) 38.
- [5] M.E.S. Hegarty, A.M. O'Connor, J.R.H. Ross, *Catal. Today* 42 (1998) 225.
- [6] J.A. Lercher, J.H. Bitter, W. Hally, W. Niessen, K. Seshan, *Stud. Surf. Sci. Catal.* 101 (1996) 463.
- [7] S. Wang, G.Q. Lu, *Energy Fuels* 12 (1998) 248.
- [8] A.M. Gadalla, B. Bower, *Chem. Eng. Sci.* 42 (1988) 3049.
- [9] Z.-W. Liu, H.-S. Roh, K.-W. Jun, H.S. Potdar, M. Ji, *J. Ind. Eng. Chem.* 9 (2003) 576.
- [10] Z.-W. Liu, H.-S. Roh, K.-W. Jun, *J. Ind. Eng. Chem.* 9 (2003) 267.

- [11] H.-S. Roh, K.-W. Jun, S.-C. Baek, S.-E. Park, *Bull. Kor. Chem. Soc.* 23 (2002) 1166.
- [12] H.-S. Roh, K.-W. Jun, S.-C. Baek, S.-E. Park, *Catal. Lett.* 81 (2002) 147.
- [13] H.-S. Roh, K.-W. Jun, S.-C. Baek, S.-E. Park, *Bull. Kor. Chem. Soc.* 23 (2002) 793.
- [14] S.-H. Seok, S.H. Han, J.S. Lee, *Appl. Catal. A* 215 (2001) 31.
- [15] S.-H. Seok, S.H. Choi, E.D. Park, S.H. Han, J.S. Lee, *J. Catal.* 209 (2002) 6.
- [16] T. Kim, S. Moon, S.-I. Hong, *Appl. Catal. A* 224 (2002) 111.
- [17] A. Trovarelli, C. de Leitenburg, G. Docetti, *Chemtech* 27 (1997) 32.
- [18] J. Kaspar, P. Fornasiero, M. Graziani, *Catal. Today* 50 (1999) 285.
- [19] S. Rossignol, F. Gerard, D. Duprez, *J. Mater. Chem.* 9 (1999) 1615.
- [20] M. Thammachart, V. Meeyoo, T. Risksomboon, S. Osuwan, *Catal. Today* 68 (2001) 53.
- [21] C. de Leitenburg, A. Trovarelli, J.L. Lorea, F. Cavani, G. Bini, *Appl. Catal. A* 139 (1996) 161.
- [22] P. Bera, K.C. Patil, V. Jayaram, G.N. Subbanna, M.S. Hegde, *J. Catal.* 196 (2000) 293.
- [23] G. Balducci, J. Kaspar, P. Fornasiero, M. Grazini, *Catal. Today* 101 (1997) 1750.
- [24] E. Bekyarova, P. Fornasiero, J. Kaspar, M. Graziani, *Catal. Today* 45 (1998) 178.
- [25] D. Terribile, A. Trovarelli, C. de Leitenburg, A. Primareva, G. Dolcetti, *Catal. Today* 47 (1999) 133.
- [26] X. Li, J.-S. Chang, S.-E. Park, *Chem. Lett.* (1999) 1099.
- [27] X. Li, J.-S. Chang, M. Tian, S.-E. Park, *Appl. Organomet. Chem.* 15 (2001) 109.
- [28] J.A. Montoya, E. Romero-Pascual, C. Gimon, P.D. Angel, A. Monzon, *Catal. Today* 63 (2000) 71.
- [29] J. Macek, M. Marinsek, *Nanostruct. Mater.* 12 (1999) 499.
- [30] H.S. Potdar, H.-S. Roh, K.-W. Jun, M. Ji, Z.-W. Liu, *Catal. Lett.* 84 (2002) 95.
- [31] W.-S. Dong, H.-S. Roh, K.-W. Jun, S.-E. Park, Y.-S. Oh, *Appl. Catal. A* 226 (2002) 63.
- [32] A. Cabanas, J.A. Darr, E. Lester, M. Poliakoff, *J. Mater. Chem.* 11 (2001) 561.
- [33] P. Fornasiero, R.D. Monte, R.G. Rao, J. Kaspar, S. Meriani, A. Trovarelli, M. Graziani, *J. Catal.* 151 (1995) 168.
- [34] ASTM Card No. 4-0835.
- [35] H.-S. Roh, K.-W. Jun, W.-S. Dong, S.-E. Park, Y.-S. Baek, *Catal. Lett.* 74 (2001) 31.
- [36] G.K. Chuan, S. Jaenicke, *Appl. Catal. A* 163 (1997) 261.
- [37] C.E. Hori, H. Permana, K.Y. Simon, A. Brenner, K. More, K.M. Rannnoeller, D. Belton, *Appl. Catal. B* 16 (1998) 105.